
Article:
East, Jessica L. H., Hume, Emma, Lancaster, Kate orcid.org/0000-0002-0045-9909 et al. (2 more authors) (2020) Hydrodynamic motion of guiding elements within a magnetic switchyard in fast ignition conditions. Physics of Plasmas. 062701. ISSN 1089-7674

https://doi.org/10.1063/5.0002156

Hydrodynamic Motion of Guiding Elements within a Magnetic Switchyard in Fast Ignition Conditions

J. L. H. East[1], E. J. Hume[2], K. L. Lancaster[2], A. P. L. Robinson[3], and J. Pasley[2*]

[1] *Department of Physics, The University of York, Heslington, York, YO10 5DD, U.K.*

[2] *York Plasma Institute, Department of Physics, The University of York, Heslington, York, YO10 5DQ, U.K. and*

[3] *Central Laser Facility, STFC Rutherford Appleton Laboratory, Harwell Campus, Didcot, OX11 0QX, U.K.*

Magnetic collimation via resistivity gradients is an innovative approach to electron beam control for the cone-guided fast ignition variant of inertial confinement fusion. This technique uses a resistivity gradient induced magnetic field to collimate the electron beam produced by the high-intensity laser-plasma interaction within a cone-guided fast ignition cone-tip. A variant of the resistive guiding approach, known as the "magnetic switchyard", has been proposed which uses shaped guiding elements to direct the electrons toward the compressed fuel. Here the 1D radiation-hydrodynamics code HYADES is used to investigate and quantify the gross hydrodynamic motion of these magnetic switchyard guiding elements in conditions relevant to their use in fast ignition. Movement of the layers was assessed for a range of two-layer material combinations. Based upon the results of the simulations a scaling law is found that enables the relative extent of hydrodynamic motion to be predicted based upon the material properties of the switchyard, thereby enabling optimization of material-combination choice on the basis of reducing hydrodynamic motion. A multi-layered configuration, more representative of an actual switchyard, was also simulated in which an outer Au layer is employed to tamp the motion of the outermost guiding element of the switchyard.

I. INTRODUCTION

Fast ignition[1] (FI) is an Inertial Confinement Fusion (ICF) ignition concept in which the ignition of the thermonuclear fuel occurs independently of the implosion process. The fuel is first imploded to high densities (hundreds of g cm^{-3}), followed by an interaction with a high energy laser, having a pulse duration on the order of 10-20 ps and focused intensity on the order of 10^{20} W/cm^2, to generate an intense burst of relativistic electrons which act to heat the fuel to ignition temperatures. In re-entrant cone-guided FI a hollow cone with a closed tip is employed to bring the region of electron generation as close as is practicable to the dense imploded fuel[2].

A significant problem with cone-guided FI is the divergence of the high-energy electrons that emerge from the cone into the fuel plasma. The divergence reduces the coupling efficiency between the ignitor laser beam and the compressed fuel. Experimental studies suggest that relativistically intense laser interactions ($I > 10^{19}$ W/cm^2) with solid targets produce a fast electron beam with a divergence angle of 30° or more[3–5]. A hybrid PIC code was used to investigate the effect of electron beam divergence on the required ignition energy for a cone-guided FI configuration as part of a parametric study[6]. Beam collimation in the target plasma was found to decrease with increasing initial divergence angle of the injected electron beam; consequently, the required electron beam energy for ignition increased rapidly with divergence angle. These results suggest that achievement of ignition through FI may require excessive short-pulse laser energy. One possible solution to this problem is to control the electron beam direction and divergence. The use of vacuum gaps was proposed to collimate the electron beam by inducing a radial electric field[7]. A further approach employed a carbon wire attached to the end of a hollow cone to guide the energetic electrons[8]. Further

*Electronic address: john.pasley@york.ac.uk

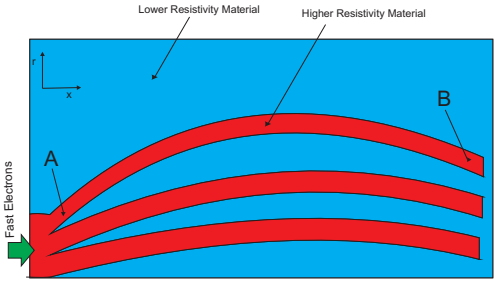

FIG. 1: Schematic of the magnetic switchyard configuration. Fast electrons enter the switchyard at point A, and are directed by the guiding elements to a small volume at point B.

work is required to determine whether such a device could survive the extreme conditions involved in an implosion.

The idea of using resistivity gradients to collimate the fast electron beams by means of a self-applied magnetic field was first proposed in 2007[9]. Substitution of Ohm's Law, $\mathbf{E} = -\eta \mathbf{j}_f$, into Faraday's Law, $\nabla \times \mathbf{E} = \frac{\partial \mathbf{B}}{\partial t}$, yields

$$\frac{\partial \mathbf{B}}{\partial t} = \nabla \eta \times \mathbf{j}_f + \eta \nabla \times \mathbf{j}_f \tag{1}$$

where $\mathbf{B}$ is the induced magnetic flux density, $\mathbf{j}_f$ is the fast electron current density and η is resistivity of the target material. The first term drives electrons to areas of higher resistivity, generating the desired collimating magnetic field. This is then reinforced by the second term, which generates a magnetic field that drives the fast electrons towards regions of higher $\mathbf{j}_f$. In the work by Robinson and Sherlock suitably collimating resistivity gradients were generated by surrounding a high resistivity cylindrical filament with a cladding of lower resistivity material. Experiments performed at Vulcan PetaWatt demonstrated that electron divergence was reduced by the resistivity gradient induced between adjacent regions of Al and Sn[10,11]. Further experimental results[12] demonstrated that an electron beam could be collimated in a cylindrical system, with resistivity gradients creating an azimuthal magnetic field.

A further development of the resistivity gradient induced magnetic collimation scheme has been proposed to collimate the fast electron beam in what is called a "magnetic switchyard"[13]. The magnetic switchyard structure has multiple thin guiding elements curved to direct the electrons into a small volume as depicted in Figure 1. Each single guiding element will trap fast electrons coming into the switchyard with a small range of divergence angles. The electrons will leave the element with a similar degree of collimation, however the use of curved elements means the electron beam path will be directed towards the dense fuel. The use of multiple guiding elements ensures that a significant proportion of the fast electrons are controlled by the magnetic fields generated in the switchyard.

In this paper we investigate the extent to which Ohmic heating can cause expansion of the guiding elements. Such expansion is to be expected, in part due to the temperature gradients induced by the differential Ohmic heating, but also given the fact that the filament material is usually of higher Z than the surrounding low resistivity material[11]. If the guiding centre expands then the current density is liable to decrease thus reducing the term of Equation 1, affecting the Larmor radius of the fast electrons, and resulting in possible loss of high energy electron confinement. The extent of guiding element expansion is therefore assessed for a range of different material combinations to quantify the significance of material choice in the observed hydrodynamic motion. A clear relationship is seen between the mass density of the layers and the observed inter-layer boundary shift under various degrees of heating, from which a scaling law is identified.

II. SIMULATIONS AND DISCUSSION

The radiation-hydrodynamic code HYADES[14] is used to examine the hydrodynamic evolution of the guiding elements in the magnetic switchyard scheme during the time period in which it must guide the energetic electrons. In this study a 1D cylindrical geometry is used. A multigroup diffusion description is employed to emulate radiation transport, and conduction is handled by a flux-limited diffusion approximation. It has previously

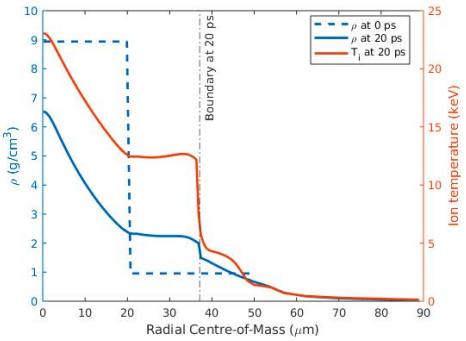

FIG. 2: Mass density contours in a cylindrical collimator comprised of two regions at simulation time t = 0 ps and 20 ps and the ion temperature profile at 20 ps. The inner region is composed of Cu and and the outer CH_2.

been shown that the MHD effects induced by the passage of FI relevant beams of energetic electrons are small by comparison to the effects of material pressure[15].

Different material combinations are simulated for a two-layer magnetic switchyard configuration. As appropriate to the magnetic guiding schemes under consideration, the innermost region is always of comparatively higher high-temperature-resistivity. The behaviour of eight material combinations were examined; C-CH_2, Al-CH_2, Cu-CH_2, Al-C, Ti-C, Cu-C, Ti-Al and Cu-Al, here presented in order inner - outer layer. The initial thickness of the inner layer is 20 μm, with the outer layer having a thickness of 30 μm. The intention here is to simulate a single cylindrical guiding element surrounded by material. In the original magnetic switchyard concept the guiding elements were suggested to be ~ 10 μm thick. Here a 20 μm inner layer thickness is employed, which is both comparable to the anticipated dimensions that might be employed in practice and also sufficiently thick that the initial thickness of the layer does not become a determining factor in the dynamics on the time-scales of interest.

The rates of energy deposition in the guiding elements is based upon the results of the 2012 magnetic switchyard study[13]. In that investigation the temperature of the C guiding elements was found to reach $\sim$ 5 keV with the surrounding CH_2 material reaching a temperature of $\sim$ 1 keV using the Hybrid-PIC simulation code ZEPHYROS[10,12]. In the present study, energy deposition rates for these same two materials are found so as to attain comparable temperatures in a HYADES simulation. The heating rates so derived are 3.61×10^{20} J/g·s and 8.88×10^{19} J/g·s for the inner and outer regions respectively. These heating rates are held constant throughout the HYADES simulation, and cause the temperatures to equilibrate to those found in the earlier study. These heating rates are somewhat higher than the average ohmic heating rates found in the electron transport calculations, though they agreed to within 30%. This is to be expected since HYADES incorporates a more detailed description of radiative loss terms than ZEPHYROS, and so to achieve comparable temperatures requires increased energy input. To ensure that our results cover the whole of the relevant parameter space further simulations are performed in which the heating rate is varied by a factor of four, from 0.5 to 2.0 of the heating rates stated here. The same heating rates are applied to all material combinations employed in the study so as to isolate the effect of the hydrodynamic properties of the guiding materials on the hydrodynamic behaviour of the switchyard. All materials are described using an average-atom LTE ionisation model and SESAME equations of state.

Figure 2 is an example of the mass density and temperature profiles for the Cu-CH_2 layer configuration. Over the course of the simulation the differential heating and ionisation results in higher pressures in the central cylinder compared to the outer layer, causing the inner region to expand rapidly. As the velocity of the interface rises above the local speed of sound in the outer region a shock front forms[16] (seen at around 38 μm for the t = 20 ps case).

The shift of the region boundary is then found for each material combination. Figure 3a demonstrates that the boundary shift is approximately proportional to the ratio of the pressure difference between the two material re-

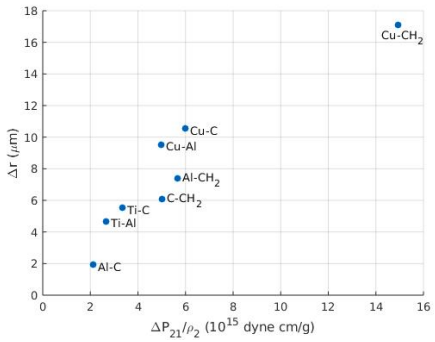

(a)

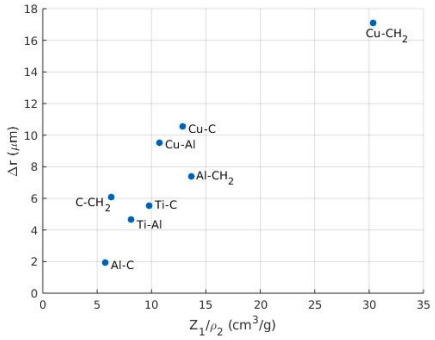

(b)

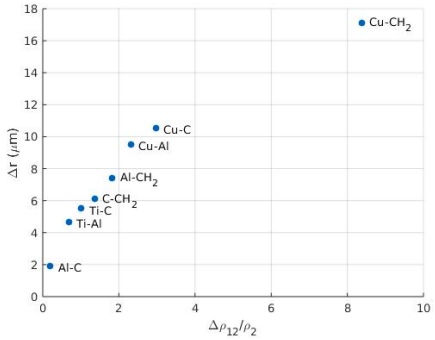

(c)

FIG. 3: Dependence of region boundary shift at 20 ps on various initial properties of the system. Boundary shift is plotted against: (a) pressure difference between the inner and outer layers; (b) Z of the inner layer material; and (c) mass density difference between the inner and outer layers. All x-axis parameters have been normalised by the mass density of the material in the outer layer.

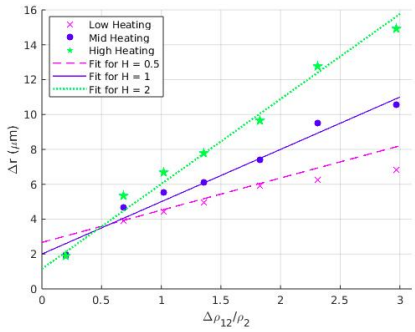

FIG. 4: Shift of the region boundary observed at 20 ps as a function of initial density difference between layers. Results are shown for three heating rates, where mid heating represents the original heating rate, low heating is a factor 2 lower and high heating is a factor 2 greater.

gions and the mass density of the outer region, consistent with Newton's second law. Assuming total ionisation of both regions, the pressure will be roughly proportional to the atomic number. Displacement of the boundary against the ratio of the central material Z to the outer material mass density is shown in Figure 3b; the approximately linear trend observed is indicative of the pressure in the inner region being dominant in the interaction. The observation that a lower-Z combination yields lower boundary shift and is the preferred choice from a hydrodynamic standpoint is encouraging, as the use of high-Z materials in structured collimator devices results in greater angular scattering of fast electrons which is disruptive to guiding.

Figure 3c indicates the dependence of the shift on the difference in density between the materials in each region, $\Delta\rho_{12} = \rho_1 - \rho_2$ where ρ_1 and ρ_2 are the densities of the high and low resistivity materials respectively. The greatest shift corresponds to the greatest mass density difference, Cu-CH_2, with a 17.1 μm shift, and the smallest shift corresponds to the smallest density difference, Al-C, with a 1.9 μm shift.

To ensure that the study covers the whole of the relevant parameter space, simulations are repeated for all material combinations (excluding Cu-CH_2, since this is

already shown to be anomalous) with energy deposition set at either 0.5 or 2.0 times the original heating rate. The boundary shifts are found as a function of the density difference between the layers as shown in Figure 4. A general fit is found for these results where the boundary shift observed is found to scale with the mass density of the layers and time as,

$$\Delta r \approx 0.15 t_{ps} H^{0.7} \left(\frac{\Delta \rho_{12}}{\rho_2} \right) + \frac{0.12 t_{ps} H}{0.2 + H^2} \mu m, \quad (2)$$

where the dimensionless parameter H represents a multiplier on the baseline energy deposition rate calculated for FI conditions as given earlier in this manuscript and t_{ps} represents the time in ps since the heating commenced. At low values of $\Delta\rho_{12}$ the curves for H=0.5, 1 and 2.0 are observed to cross over. Further simulations are run to verify that this prediction is physical, and it is found to be so, the explanation being as follows: The pressure in each region is proportional to the product of electron density and temperature. In the hot region of the target, the material is totally ionized (i.e. fully stripped) and so the scaling of pressure with temperature is linear going from H=0.5 to H=2.0. However in the cooler region, which in the case of H = 0.5 is at only around 500 eV, further ionisation is possible as the energy deposition rate is increased. This means that the back-pressure exerted by the cooler region will be proportionately larger at higher temperatures and hence the displacement of the boundary is reduced in absence of competing effects. At larger values of $\Delta\rho_{12}$ however, the back-pressure becomes increasingly inconsequential to the dynamics due to the dominance of the pressure in the hot region, leading to the transition in behaviour as $\Delta\rho_{12}/\rho_2$ crosses ~ 0.5 as shown in Figure 4.

Of the combinations modeled here Al-C is found to be the best two-element combination in terms of limiting the gross interface motion. Further simulations are therefore performed to test this material combination in a multi-layered geometry that is more representative of the magnetic switchyard. Both Al-C-Al-C and Al-C-Al-C-Au systems were modelled, where thicknesses of the layers were 20 μm for Al, 30 μm for C and 20 μm for Au. The Al-C-Al-C-Au combination examines the behavior of a system surrounded by a cold, dense material such as may be expected in an FI cone-tip. No external energy deposition was applied to the Au layer. In reality, some energy would be deposited in the Au by the ignitor beam, however since the Au layer is here acting to maintain the integrity of the switchyard by acting as a tamper, the case we have modelled represents a worst-case scenario. In practice the energy deposited directly into the surrounding material by the ignitor-cone interaction would act to enhance the back pressure exerted by the Au upon the outermost layer of the switchyard thereby rendering the tamping more effective. Figure 5 shows the change in the thickness of each of the regions that comprises the switchyard for the two cases modelled. The presence of the cold dense Au layer is seen to have a significant effect, with a greatly reduced expansion observed in the outermost C layer when the Au layer is included.

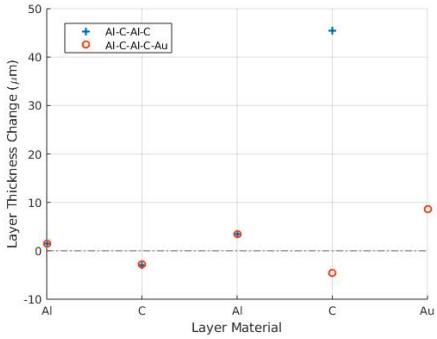

FIG. 5: The expansion or contraction of each layer in either an Al-C-Al-C or Al-C-Al-C-Au system configuration. The presence of a cold dense outer Au layer is seen to significantly affect the hydrodynamic motion of the outermost C layer.

III. CONCLUSIONS

The simulations described in this paper investigate the hydrodynamic behaviour of the guiding elements in a magnetic switchyard structure under the influence

of ignitor beam heating. It is shown that the material choice in each layer of the magnetic switchyard can strongly affect the degree of gross hydrodynamic motion observed at the boundaries of the switchyard layers. The results shown in this paper act as a guide to the extent of gross hydrodynamic motion that may be expected as a function of material choice and heating rate at different points in the heater beam interaction. A scaling law is presented which relates the boundary shift to the mass density of the layers, the energy deposition rate, and the time that has elapsed. It is also demonstrated that an Au cone-tip will effectively tamp the exterior of the switchyard even if relatively little energy is deposited in it.

ACKNOWLEDGMENTS

The authors would like to acknowledge the support of Dr Raoul Trines and Dr Robbie Scott of the STFC Rutherford Appleton Laboratory in maintaining the computing systems on which HYADES is used. Jessica East would like to acknowledge the financial backing of the STFC Rutherford Appleton Laboratory. Emma Hume was supported by the Engineering and Physical Sciences Research Council Doctoral Training Grant EP/L01663X/1. We gratefully acknowledge the HiPER project for funding the purchase of the HYADES simulation code license used in these studies. The data that supports the findings of this study is available from the corresponding author upon reasonable request.

[1] M. Tabak, J. Hammer, M. E. Glinsky, W. L. Kruer, S. C. Wilks, J. Woodworth, E. M. Campbell, M. D. Perry and R. J. Mason, *Physics of Plasmas* **1,** 1626 (1994).

[2] J. J. Honrubia and J. Meyer-ter Vehn, *Nucl. Fusion* **46**, L25 (2006).

[3] R. B. Stephens, R. A. Snavely, Y. Aglitskiy, F. Amiranoff, C. Anderson, D. Batani, S. D. Baton, T. Cowan, R. R. Freeman, T. Hall, *et al., Physical Review E* **69**, 066414 (2004).

[4] J. S. Green, V. M. Ovchinnikov, R. G. Evans, K. U. Akli, H. Azechi, F. N. Beg, C. Bellei, R. R. Freeman, H. Habara, R. Heathcote, *et al., PRL* **100**, 015003 (2008).

[5] K. L. Lancaster, J. S. Green, D. S. Hey, K. U. Akli, J. R. Davies, R. J. Clarke, R. R. Freeman, H. Habara, M. H. Key, R. Kodama, *et al., PRL* **98**, 125002 (2007).

[6] J. J. Honrubia and J. Meyer-ter Vehn, *Plasma Phys. Control. Fusion* **51**, 014008 (2009).

[7] R. B. Campbell, J. S. DeGroot, T. A. Mehlhorn, D. R. Welch, and B. V. Oliver, *Phys. Plasmas* **10**, 4169 (2003).

[8] R. Kodama, Y. Sentoku, Z. L. Chen, G. R. Kumar, S. P. Hatchett, Y. Toyama, T. E. Cowan, R. R Freeman, J. Fuchs, Y. Izawa, *et al., Nature* **432**, 1005 (2004).

[9] A. P. L. Robinson and M. Sherlock, *Phys. Plasmas* **14**, 083105 (2007).

[10] S. Kar, A. P. L. Robinson, D. C. Carroll, O. Lundh, K. Markey, P. McKenna, P. Norreys and M. Zepf, *PRL* **102**, 055001 (2009).

[11] S. Kar, D. Adams, M. Borghesi, K. Markey, B. Ramakrishna, M. Zepf, K. Lancaster, P. Norreys, A. P. L. Robinson, D. C. Carrol, *et al., J. Phys: Conf. Ser.* **244**, 022041 (2010).

[12] B. Ramakrishna, S. Kar, A. P. L. Robinson, D. J. Adams, K. Markey, M. N. Quinn, X. H. Yuan, P. McKenna, K. L. Lancaster, J. S. Green, *et al., PRL* **105**, 135001 (2010).

[13] A. P. L. Robinson, M. H. Key and M. Tabak, *PRL* **108**, 125004 (2012).

[14] J. T. Larsen and S. M. Lane, *Journal of Quantitative Spectroscopy and Radiative Transfer* **51**, 179 (1994).

[15] I. A. Bush, A. P. L. Robinson, R. Kingham and J. Pasley, *Plasma Phys. Control. Fusion* **52**, 125007 (2010).

[16] Y. B. Zel'dovich, Y. P. Raizer, W. D. Hayes and R. F. Probstein, *Physics of Shock Waves and High-Temperature Hydrodynamic Phenomena.* (Dover Publications Inc., 2002).

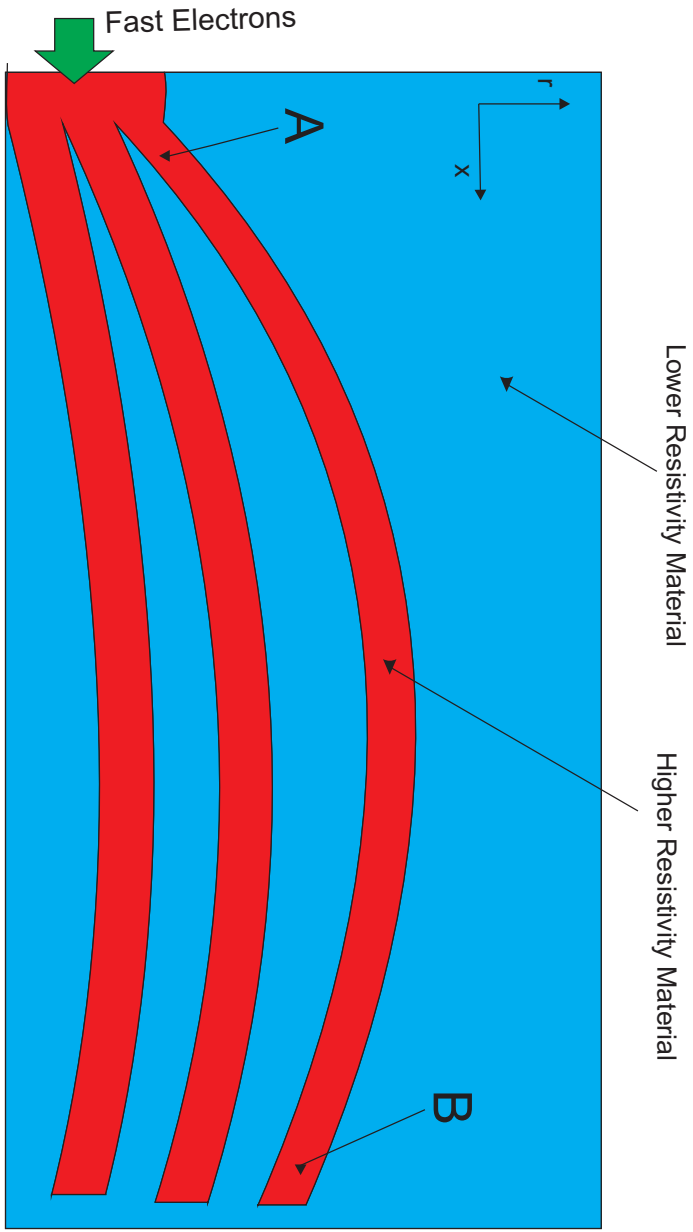

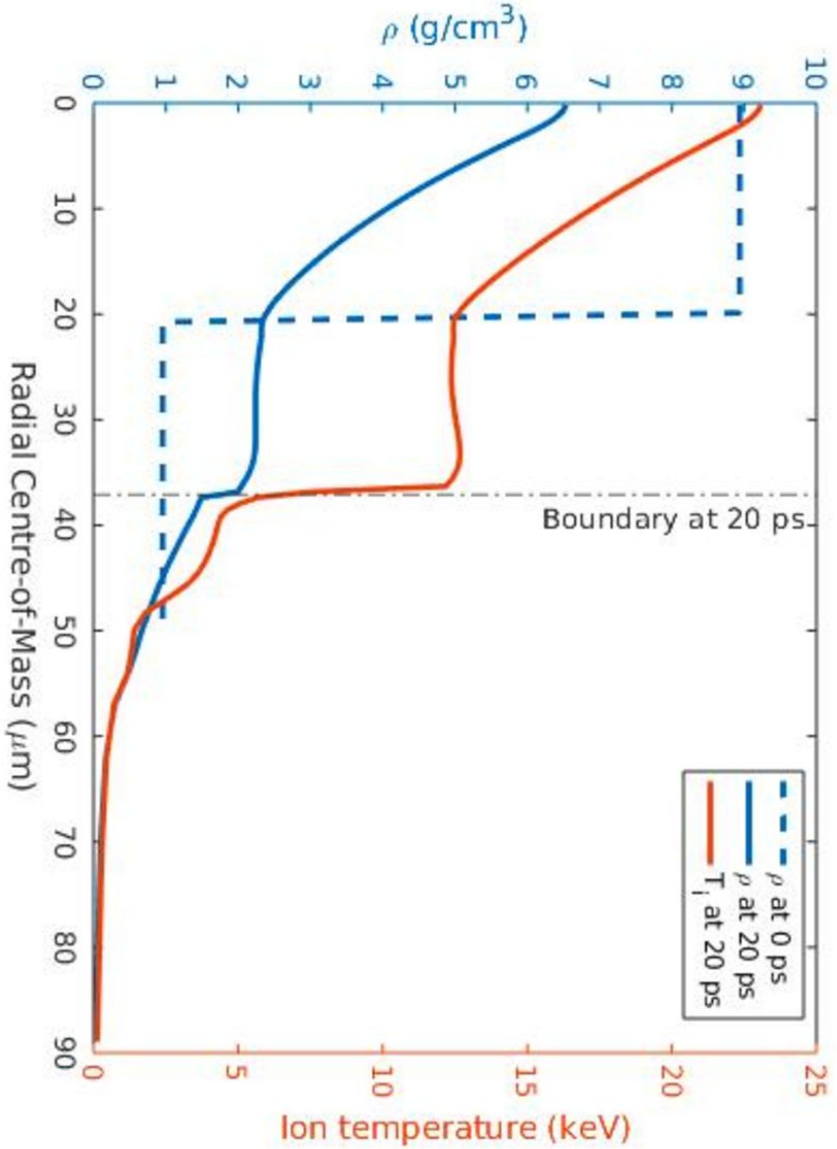

PLEASE CITE THIS ARTICLE AS DOI: 10.1063/5.0002156